This study analyzed the impact factors in an extreme precipitation event that occurred during July 2023 in Beijing, based on the Weather Research and Forecasting (WRF) model. Several experiments were selected to assess the impacts of topography and land use, with examining the causes of the event and the related mechanisms. It concludes that topographical features caused the uplift of air masses in the mountainous regions leading to significant enhancement of the convective intensity over Beijing and precipitation for a prolonged duration. The presence of urban surfaces contributed to reductions in the latent heat flux and wind speed, resulting in decreased energy transfer to the southwestern mountainous regions via easterly winds. This study is interesting and the manuscript is well written. There are some issues that could be addressed to improve the manuscript quality.

Response: We highly appreciate you for your thorough review and constructive comments, which significantly improve the quality of our manuscript. We have carefully considered all comments and have made the following changes.

(1) The methodological choices were better justified to enhance the scientific contribution.

(2) The water vapor budget was quantitatively assessed to improve the physical mechanism.

(3) More discussion including the ensemble simulation, the uncertainty quantification and the important limitations of our study were added.

We have also checked the English texts carefully and corrected the grammatical errors through the manuscript. Below we indicate the comments and use blue font for our responses. We hope the following point-to-point response could address your concern.

Introduction: This part is generally coherent and logical, but there are some expression issues that need improvement.

Lines 57-59: The last sentence is related to the effect of surface roughness induced by cities. Therefore, it better remove this to the paragraph of introducing urbanization.

Response: Thanks for your comments. Revisions have been made as suggested.

Line 79: … another key factors …., since the authors have pointed out topography as one of the most important factors.

Response: We have revised the manuscript to make the expression explicitly.

Lines 82-83: Delete "which significantly increases the surface roughness". Urban heat island can cause convergence and upward lifting in the lower atmosphere, but is not the cause of surface roughness.

Response: Thanks for your comments. The description in the original text is indeed ambiguous, which has been deleted.

Lines 87: Delete "modifying".

Response: Revised.

Lines 102-103: This sentence introduces the research area, but the expression is not coherent and needs to be revised.

Response: The sentence has been revised to "Beijing is located in the northwest edge of the North China Plain, where is the transitional zone between the Taihang Mountains, Yanshan Mountains, and North China Plain."

Experimental Design:

The WRF simulation is carried out on 49 vertical layers and the upper boundary was set as 50 hPa. Is there any evidence or literature supported this setting?

Response: Thanks for your comments. Previous sensitivity studies have demonstrated

that the number of vertical levels in WRF significantly influences the representation of vertical atmospheric structures (Jenney et al. 2023, Jiang and Hu 2023). It is apparent that the finer vertical resolution can enhance the accuracy in representing the extreme precipitation process. However, an excessively large number of vertical levels would substantially increase computational costs. Therefore, a configuration with 49 vertical levels was adopted, which improves the simulation accuracy while ensuring computational efficiency and timely output of the simulation results.

The reason why we configure the upper boundary at 50hPa is to resolve the vertical structure of the subtropical high and upper-level jet streams while minimizing spurious wave reflection near the upper boundary. The value is standard and can be seen in other researches on extreme precipitation events (Wang et al. 2018, Yu et al. 2024, Pei et al. 2025).

We have added this explanation to the method section in the revised version.

Results:

Line 225: Is “EP” shorted for “extreme precipition”? This abbreviation is only used once and need be changed.

Response: Sorry for the misleading, which has been revised to the full name.

The authors state that using CMORPH data to validate the simulation results was highly reasonable, although it is an indirect observation data. The average precipitation intensity obtained from the simulations was compared with the precipitation intensity of CMORPH. Therefore, it suggests presenting the results of the statistics of MAE, RMSE and R, or at least listing them in a table.

Response: Thanks for your comments. To quantitatively evaluate the simulation accuracy of the WRF model across different study areas (D04 in the manuscript), it is divided into mountain area (where terrain height greater than 100 m) and plain area (where terrain height smaller than 100 m). The quantitative statistics were listed in Table 2 in the revised version. The more explanations are added as follows.

Table 1: Statistics of the precipitation intensity between simulations and CMORPH data.

	R	RMSE	MAE
All	0.743	2.001	1.648
Mountain	0.812	2.096	1.771
Plain	0.560	1.169	0.949

It shows that, the correlation coefficient (R = 0.56) of the plain areas shows a smaller value compared with the two aforementioned datasets (R = 0.74 and 0.81, respectively). For the result of MAE and RMSE, the statistics in the plain areas are significantly superior to those in the mountainous areas and the entire study region. This may be due to that there are more stations in the plain areas, and the precipitation is smaller than mountain areas.

For the physical mechanism of this precipitation event, the authors can focus on the water vapor transport, especially the differences in water vapor budget at each of the boundary.

Response: Thanks for your comments. We realized that the results can be more convincing, with the quantitative calculation of moisture budget analysis. Following suggestion form you and the first reviewer, the quantitative water vapor flux were listed in Table 3.

Table 2: The water vapor flux (kg/(m s)) during each period for different schemes.

Time	Scheme	North	South	Zonal	East	West	Meridional	Net
T1	LU_2020	58.63	-19.52	39.11	130.50	-100.61	29.89	69.00
	LU_nohgt	78.89	-83.09	-4.20	141.79	-110.93	30.86	26.66
	LU_nourb	55.42	-22.42	33.00	133.97	-94.19	39.78	72.78
T2	LU_2020	146.94	-109.39	37.55	146.05	-160.02	-13.97	23.58
	LU_nohgt	222.99	-146.99	76.00	176.09	-199.31	-23.22	52.78
	LU_nourb	152.31	-113.83	38.48	139.02	-150.29	-11.27	27.21
T3	LU_2020	199.32	-169.36	29.96	71.65	-95.36	-23.71	6.25
	LU_nohgt	228.22	-237.85	-9.63	32.12	-0.69	31.43	21.80
	LU_nourb	206.16	-160.40	45.76	74.65	-64.38	10.27	56.03

In addition, in order to enable readers and reviewers to more clearly discern the variations in moisture transport from different boundaries, The corresponding figures (Figures 8 and 9 in the initial version) was reproduced. In these new figures, positive moisture flux denotes the transport of water vapor into the region, whereas negative

values indicate the export of water vapor from the region. The corresponding texts were revised to make the results quantitatively explicit.

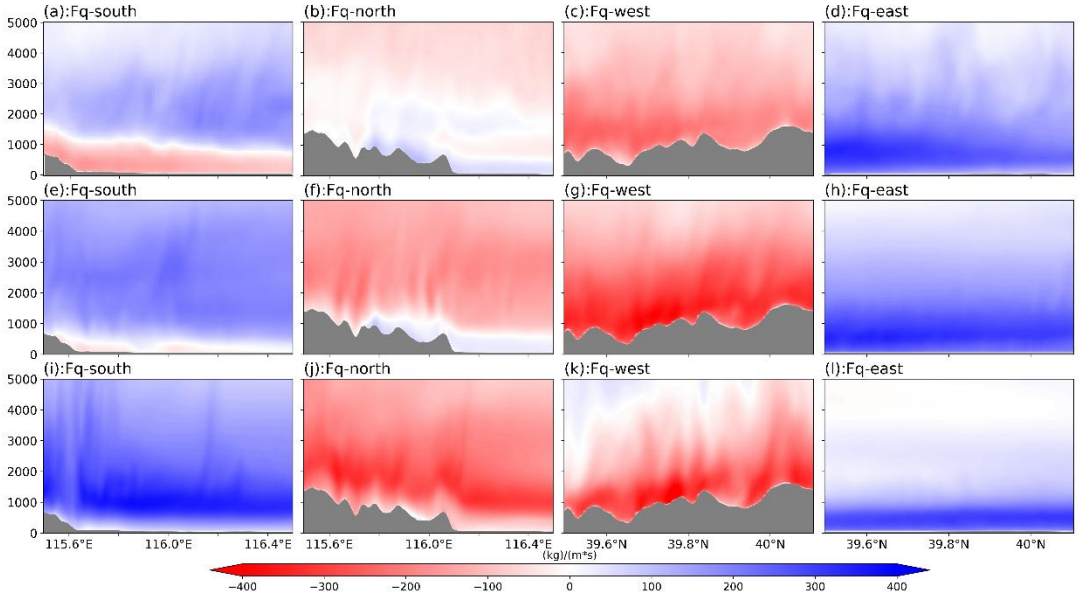

Figure 8. Distribution of water vapor flux magnitude in the LU_2020 scheme across latitude-height/longitude-height coordinates of RegP. Figures show the water vapor flux magnitude for time periods T1 (a – d), T2 (e – h), and T3 (i – l), with fluxes from the south (a, e, i), north (b, f, j), west (c, g, k), and east (d, h, l). Positive and negative water vapor flux values correspond to input and output water vapor flux relative to RegP.

Figure 8 shows the magnitudes of the water vapor flux at the four boundaries of region RegP for LU_2020. An increase in net moisture convergence during each period leads to higher precipitable water over the region, which in turn provides more favorable conditions for precipitation over study region. Specifically, the moisture inflow across the southern boundary (Figure 8a, e, i) and the eastern boundary (Figure 8d, h, l) represents meridional and zonal sources of water vapor entering the region. The outflow across the northern boundary (Figure 8a, e, i) and the western boundary reflects the moisture exported from the region. The difference between the inflow and outflow moisture flux indicates net moisture income in each time period (shown in Table 2).

During period T1, about 49.58 kg/(m s) water vapor was transported southward at lower latitudinal levels along the southern boundary, while it was transported northward at high latitudes (in total 58.63 kg/(m s) northward). As the Taihang

Mountains extend in a southwest-northeast direction in the study area, the eastern zonal airflow (in total 130.50 kg/(m s)) blocked by the Mountainous area and shifted southward which explained why water vapor was transported southward in northern boundary. Overall, at T1, the moisture input into the region was dominated by zonal water vapor transport. Although the meridional transport contributed a relatively large amount of moisture inflow, its substantial outflow resulted in a comparatively smaller net contribution to the regional moisture budget.

During periods T2 and T3, the water vapor flux distributions were similar between the two periods, while the magnitude of water vapor decreased in period T3 (from 23.58 kg/(m s) to 6.25 kg/(m s)). Although the zonal water vapor transport increased to some extent, the total moisture inflow during the two periods remained comparable. Meridionally, the eastward water vapor flux also decreased from T2 to T3 (from -13.97 kg/(m s) to -23.71 kg/(m s)). In addition, the water vapor transport during T3 became more concentrated in the lower layers which indicate the contribution of low-level water vapor transport to the precipitation process. Compared with that in T1, the northward water vapor flux at the southern boundary was significantly increased in T2 and T3. As in T2 and T3 periods, the northwestward transport increased and lead led to strong uplift motion in the mountainous area. Consequently, the mountainous areas may have been more prone to intense convective weather events due to the sufficient water vapor and air uplift during T2 and T3.

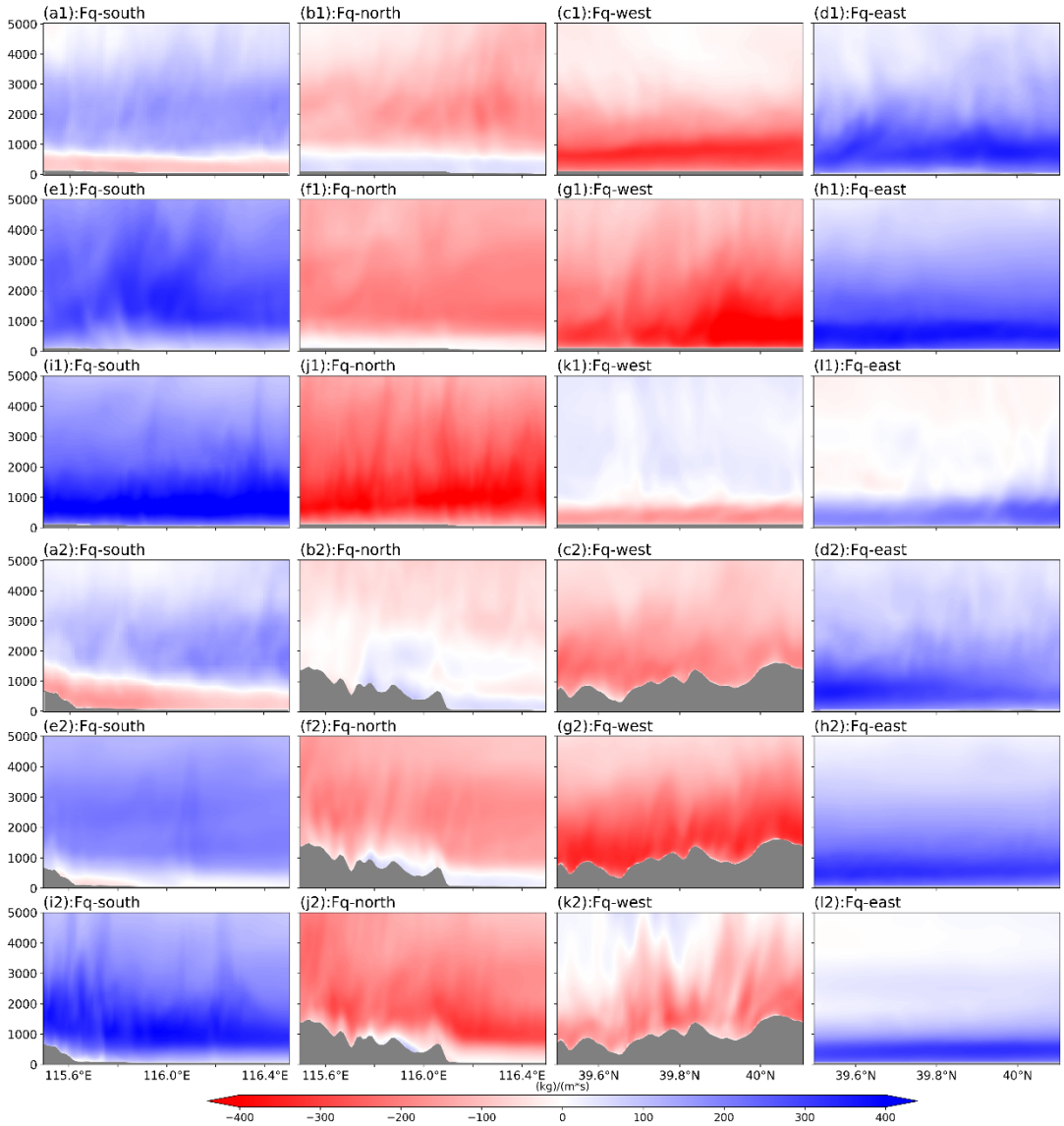

Figure 9. Water vapor fluxes as shown in Figure 8, where a1 – l1 depict the magnitude of the water vapor flux from four directions in the LU_nohgt scheme, and a2 – l2 depict the magnitude of the water vapor flux from four directions in the LU_nourb scheme.

Orographic height significantly impacted water vapor flux transport, as shown by the differences in the water vapor distribution between LU_2020 (Figure 8(a – l)) and LU_nohgt (Figure 9(a1 – l1)) and their corresponding water vapor flux transport in table 2. From a zonal perspective, orography considerably influenced the water vapor distribution within RegP. Due to orographic effects, water vapor was lifted and its northward transport was prevented, statistically reduced about 63.57 kg/(m s) in the LU_2020 (Figure 9(a1), (e1), and (i1)), which also increased the total amount of zonal water vapor flux in LU_2020. From meridional perspective, the meridional water

vapor flux output from western boundary substantially decreased during the whole period (49.41 kg/(m s) to 79.38 kg/(m s)), resulting in a noticeable rise in the water vapor content in the entire region. Furthermore, the easterly winds were blocked and diverted by the orographic effect of the mountains to the west of Beijing, which also leads to a modest increase in the magnitude of the southward water vapor flux at the southern boundary in the lower atmospheric layers.

The impacts of the urbanization on water vapor transport are shown in Figure 9(a2 – l2). There were no significant difference between LU_2020 and LU_nourb in water vapor flux during periods T1 and T2 as the difference between net convergence is smaller than 10 kg/(m s) , but during period T3, the differences mainly appeared at the western boundaries of region RegP. At the western boundary, the westward water vapor flux was 30.98 kg/(m s) higher compared with that in LU_nourb (Figure 9(k2)). These differences of moisture flux between different schemes were mainly due to wind speed in lower troposphere. As urban land use can influence local atmospheric circulation, such strong ascent induces horizontal convergence and a subsequent conversion of horizontal momentum into vertical motion. Such momentum redistribution can reduce the horizontal wind speed, particularly within the convectively active region, leading to a reduction in moisture flux across the western and northern boundaries.

Discussion:

This study involved the main physics schemes based on the model configurations listed in Table 1. It is recommended to analyze the limitations of this study, or the impacts of different physics schemes.

Response: Thanks for your comments. We admitted that, physical parameterization options have significant influences on precipitation simulations, not only for the magnitude and duration, but also for spatial and temporal distribution. The parameterization method adopted in this study had also been used in other studies about urban extreme precipitation events (Ryu et al. 2016, Wang et al. 2018, Luo et al. 2023, Wang et al. 2023, Xian et al. 2023), which can partly can prove the rationality

of this study. Following your suggestion, the model uncertainty was further accessed using an ensemble simulation of LU_2020 scheme, where are originated from ensemble members of ERA5. They provide estimates of the short-range forecast uncertainty, and can be considered to represent the evolution of the errors in the high-resolution component of ERA5 (Hersbach et al. 2020). The results were shown in Supplementary Figure S4 and the following tests were added in the revised version.

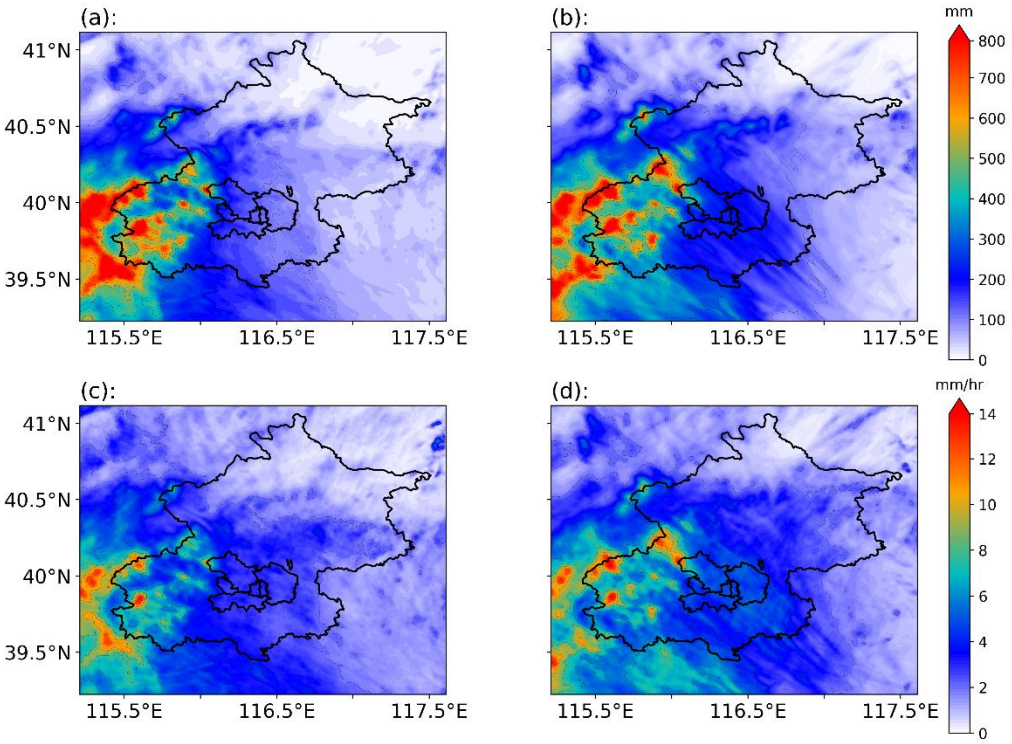

Figure S4: Comparison between simulated results of the events. (a), (b) represents the accumulated precipitation amount of LU_2020 experiment and 10 member ensemble mean, while (c), (d) represents the corresponding intensity simulation, respectively.

The results show that there is slightly difference between the ensemble mean simulation and our experimental results (Figure S4). Statistically, the average precipitation intensity is 3.6 mm/hr for LU_2020 scheme and 4.1 mm/hr for the ensemble mean. The RMSE and MAE of precipitation intensity is 1.17 mm/hr and 0.86 mm/hr for the two simulation results and the correlation coefficient is 0.90. Therefore, the experimental scheme and simulation results in this study are convincing. We have added this discussion in the revised version.

Again, thanks for your thorough review and valuable comments.

The references in our response are listed as follow. Some of them are already in the manuscript, while others are newly added.

References

1. Hersbach, H., B. Bell, P. Berrisford, et al. (2020). "The ERA5 global reanalysis." *Quarterly Journal of the Royal Meteorological Society* **146**(730): 1999-2049.
2. Jenney, A. M., S. L. Ferretti and M. S. Pritchard (2023). "Vertical Resolution Impacts Explicit Simulation of Deep Convection." *Journal of Advances in Modeling Earth Systems* **15**(10): e2022MS003444.
3. Jiang, L. and J. Hu (2023). "Influence of the lowest model level height and vertical grid resolution on mesoscale meteorological modeling." *Atmospheric Research* **296**: 107066.
4. Luo, Y., J. Zhang, M. Yu, et al. (2023). "On the Influences of Urbanization on the Extreme Rainfall over Zhengzhou on 20 July 2021: A Convection-Permitting Ensemble Modeling Study." *Advances in Atmospheric Sciences* **40**(3): 393-409.
5. Pei, L., S.-G. Miao, X.-Y. Huang, et al. (2025). "Assessing the added value of convection-permitting modeling for urban climate research: A case study in eastern China." *Advances in Climate Change Research* **16**(1): 1-11.
6. Ryu, Y.-H., J. A. Smith, E. Bou-Zeid, et al. (2016). "The Influence of Land Surface Heterogeneities on Heavy Convective Rainfall in the Baltimore–Washington Metropolitan Area." *Monthly Weather Review* **144**(2): 553-573.
7. Wang, J., J. Feng and Z. Yan (2018). "Impact of Extensive Urbanization on Summertime Rainfall in the Beijing Region and the Role of Local Precipitation Recycling." *Journal of Geophysical Research: Atmospheres* **123**(7): 3323-3340.
8. Wang, J., S. Miao, Q.-V. Doan, et al. (2023). "Quantifying the Impacts of High-Resolution Urban Information on the Urban Thermal Environment." *Journal of Geophysical Research: Atmospheres* **128**(6): e2022JD038048.
9. Xian, T., J. Guo, R. Zhao, et al. (2023). "The Impact of Urbanization on Mesoscale Convective Systems in the Yangtze River Delta Region of China: Insights Gained From Observations and Modeling." *Journal of Geophysical Research: Atmospheres* **128**(3): e2022JD037709.
10. Yu, H., A. F. Prein, D. Qi, et al. (2024). "Kilometer-scale multi-physics simulations of heavy precipitation events in Northeast China." *Climate Dynamics* **62**(9): 9207-9231.